Published in "Molecular Physics 115(14): 1691–1699, 2017"
which should be cited to refer to this work.

Shear-induced migration in colloidal suspensions

Philip Marmet, Alberto Scacchi and Joseph M. Brader

Department of Physics, University of Fribourg, Fribourg, Switzerland

ABSTRACT

Using Brownian dynamics simulations, we perform a systematic investigation of the shear-induced migration of colloidal particles subject to Poiseuille flow in both cylindrical and planar geometry. We find that adding an attractive component to the interparticle interaction enhances the migration effect, consistent with recent simulation studies of platelet suspensions. Monodisperse, bidisperse and polydisperse systems are studied over a range of shear-rates, considering both steady-states and the transient dynamics arising from the onset of flow. For bidisperse and polydisperse systems, size segregation is observed.

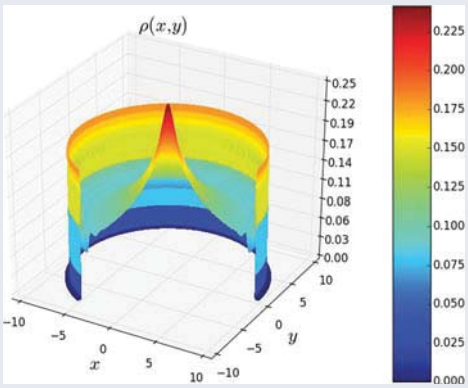

KEYWORDS

Colloidal suspensions; migration; size segregation; poiseuille flow

1. Introduction

Soft materials, such as colloidal suspensions, display a wide range of response to externally applied deformation. Even in the case of simple shear flow one can observe nonlinear rheological phenomena such as shear thinning, shear thickening and yielding [1], as well as shear-induced spatial inhomogeneities, such as shear banding [2–5] or lane formation [6,7]. Simple shear is characterised by a translationally invariant shear-rate, reflecting the fact that only the relative velocity of a colloid with respect to its surroundings is of physical relevance, but can nevertheless generate interesting flow instabilities, such as those arising from shear gradient-concentration coupling in dense systems [3–5]. Situations for which the shear-rate is a function of position are in general less well understood, because the spatially dependent shear-rate couples in a complicated way to both the density and stress in the nonequilibrium system.

In addition to the aforementioned phenomena, an important new physical mechanism is present in systems with a spatially varying shear-rate: shear-induced migration. If the shear-rate varies significantly on the scale of a colloid diameter, then the particles undergo a biased diffusion which causes them to drift ('migrate') to regions of lower shear gradient. The migration of colloids in channel flow is a dominant transport mechanism in suspensions, which has been exploited to facilitate segregation in colloidal mixtures [8,9] and which is relevant for understanding the flow of blood [9] as well as for numerous applications, such as food processing [10]. Moreover, microfluidic devices in which small quantities of fluid are driven through a microchannel are an emerging technology for processing suspensions (e.g. pharmaceuticals).

The present understanding of migration physics has its origins in the 1980 study of Gadala-Maria and Acrivos [11], who performed viscosity measurements on a suspension of large (non-colloidal) spheres using a

CONTACT Alberto Scacchi alberto.scacchi@unifr.ch

Couette rheometer. For volume fractions above approximately 30% they observed an anomalous drift in the measured viscosity as a function of time, which eventually saturated to a reproducible steady-state value. It was only several years later that Leighton and Acrivos proposed a microscopic mechanism for the observed time-dependence of the viscosity [12]. They realised that for flows with a spatially dependent shear-rate the collision frequency of a particle with its neighbours is not isotropically distributed over the surface of the particle the surface regions subject to a higher shear-rate will experience on average a greater number of collisions than those subject to a lower shear-rate. This leads on sufficiently large time-scales to a biased diffusive motion. For the Couette rheometer employed by Gadala-Maria and Acrivos [11], a shear gradient can be found in the region between the bottom of the rotating cylinder and the (static) fluid reservoir underneath it. This drives a steady migration of particles from the gap between the two Couette cylinders into the reservoir, a process which continues until the migration flux is balanced by the flux due to the particle concentration gradient.

Following the original phenomenological theory of Leighton and Acrivos [12] there have been a variety of theoretical, simulation and experimental studies addressing migration physics [13–20].

The earliest of these studies were the phenomenological theories of Nozieres *et al.* [13] and Phillips *et al.* [14]. The work of Phillips extended the methods of Leighton and Acrivos to enable a self-consistent determination of the density and velocity fields in a flowing suspension. More recently, microscopic density functional approaches have provided a route to calculate directly from the interparticle interaction potential the flow-induced changes in the density [6,15]. The migration of non-Brownian particles under pressure-driven flow has been simulated, using Stokesian dynamics, by Nott and Brady [16] and Morris and Brady [17]. On the experimental side, nonequilibrium density distributions have been measured using confocal microscopy by Frank *et al.* [19] and laser-Doppler velocimetry by Lyon and Leal [20]. All of the above-mentioned works focus on monodisperse systems. Bidisperse systems have been studied experimentally by Lyon and Leal [21] and by Semwogerere and Weeks [8,9], both of whom observed segregation between the two species.

In this paper, we present a systematic Brownian dynamics simulation study of particle migration in systems under Poiseuille flow. We begin by focusing on the simplest case: monodisperse repulsive-spheres. The dependence of both the steady-state density and the transient dynamics on the shear-rate is investigated and we explore the differences between cylindrical (pipe) and planar (channel) geometries, an aspect which has not yet been addressed. When considering both bidisperse and polydisperse systems we identify segregation effects, which could potentially be exploited to separate particles according to their size. Building upon these results for repulsive systems, we proceed to investigate the migration of attractive Lennard-Jones (LJ) particles, both monodisperse and polydisperse. The addition of an attractive component to the pair potential is found to significantly enhance the strength of the migration effect. With the exception of the study of Katanov *et al.* [22], in which a detailed model of blood flow was simulated, we believe that this work represents the first study of migration in systems with an attractive interaction potential.

The paper is organised as follows. In Section, 2 we give details of our Brownian dynamics simulation algorithm and in Section 3 we present the numerical results thus obtained. In Section 3.1, we consider monodisperse repulsive-spheres subject to Poiseuille flow in both cylindrical and planar (channel) geometries. Both steady-states and transient dynamics are addressed. In Section 3.2, we generalise to bidisperse and polydisperse repulsive- spheres and identify segregation effects. In Section 3.3, we consider the influence on migration of an attractive component to the pair potential, addressing the transient dynamics and steady-states of LJ particles. In Section 3.4, we generalise to polydisperse LJ spheres. Finally, in Section 4, we discuss our findings and give an outlook.

2. Numerical algorithm

We perform Brownian dynamics simulations of N particles, randomly initialised without overlap [23]. The random velocity used to generate the thermal Brownian motion is sampled from a Gaussian distribution with standard deviation $\sigma = \sqrt{2T'dt}$, where dt is the Brownian time step. The parameter T' is given by $T' = k_BT/3\pi\eta d$, where k_BT is the thermal energy, η is the fluid viscosity and d is the particle diameter. For the pipe geometry, the system is confined to a cylinder with periodic boundary conditions along the cylinder axis, whereas for the slit geometry we use periodic boundaries in the two directions parallel to the wall.

In order to model the flow of a suspension driven either down a cylindrical pipe or through a slit, we add to the random Brownian velocities a deterministic contribution taken from the Poiseuille velocity profile appropriate to the geometry of interest. For the cylindrical geometry, for example, we employ

$$v(r) = v_{\mathrm{m}}\left(1 - \left(\frac{r}{R}\right)^2\right), \qquad (1)$$

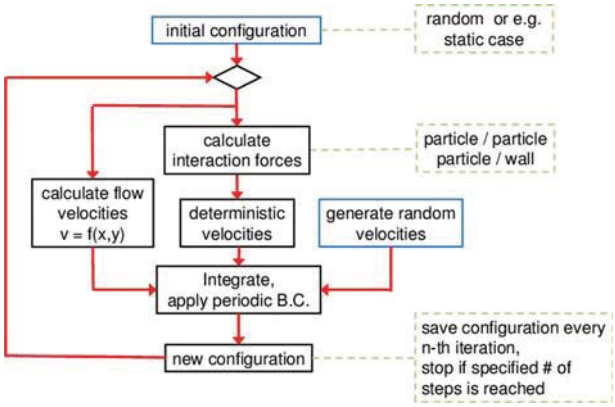

Figure 1. Schematic representation of the Brownian dynamics algorithm.

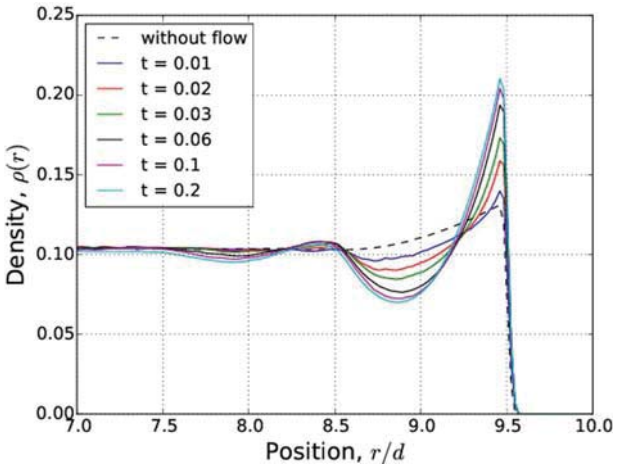

Figure 2. Density profiles at the wall for monodisperse repulsive-spheres confined by a cylindrical repulsive substrate (pipe geometry). We show the density profile for different times following the onset of Poiseuille flow at Peclet number $Pe = 250$. For increasing time, the peak at the wall is increasing.

where v_m is the maximal velocity at the centre of the pipe and R is the pipe radius. We assume that shear gradients are small on the length scale of the colloids. While using a pre-determined quadratic velocity profile to model pressure-driven flow is convenient, for finite colloidal volume fractions it represents an approximation: the nontrivial coupling between the stress, strain-rate and density fields will in reality lead to a 'blunting' of the velocity profile and thus a deviation from Poiseuille. However, provided that the colloidal volume fraction remains sufficiently low, then the deviation of the true velocity profile from the Poiseuille form will be minimal.

Fortunately for the present work, the shear-induced migration effect can be well studied within the low-volume fraction regime. We thus work with a colloidal volume fraction of $\phi = 0.05$ and, for convenience, we take the system temperature $T = 1$. For simulations performed in cylindrical geometry we will fix the pipe radius as $R = 10\,d$. All times will be given in units of the diffusion time of a single particle, namely in units of $\tau_B = d^2/D_0$, where D_0 is the bare diffusion coefficient. The steps of the numerical algorithm for our Brownian dynamics simulations are summarised schematically in Figure 1.

3. Results

3.1. Monodisperse repulsive-spheres

We study first the nonequilibrium density profile of a system of N-colloids confined in a cylindrical geometry. For simplicity, hydrodynamic interactions are neglected. The particle-particle interaction we choose to model our soft spheres is given by

$$U_{HS} = \begin{cases} 4\epsilon\left[\left(\frac{d}{r}\right)^{24} - \left(\frac{d}{r}\right)^{12} + \frac{1}{4}\right], & r \le 2^{\frac{1}{12}}d \\ 0, & r > 2^{\frac{1}{12}}d \end{cases} \qquad (2)$$

where the parameter ϵ has been set to $\epsilon = 1$. The interaction between the colloidal suspension and the confining walls is given by the potential form (2), with the radial coordinate, r, replaced by the distance between the centre of the particle and the substrate. The simulation variables have been set as follows: the number of particles $N = 400$, the Brownian time step $dt = 2 \times 10^{-5}$ and the length of the pipe $L = 13.33d$.

We first focus on the time-evolution of the average density profile from equilibrium to steady-state, following the onset of flow. In order to provide a dimensionless characterisation of the strength of the flow, we define the Peclet number as $Pe = (v_m d^2)/(RD_0)$. In Figure 2, we show the development of the density distribution close to the pipe wall as a function of density. As time progresses, the height of the first peak (closest to the wall) increases steadily before saturating to the steady-state value. This reflects an increase in the pressure acting on the wall and is a consequence of interparticle collisions pushing particles up against the confining boundary. Closely associated with the growth of the first peak is the development of an enhanced oscillatory packing structure – the flowing system has a tendency to form layers (concentric rings in the present geometry) of particles so as to minimise collisions. We note that a nonequilibrium packing structure close to the wall develops rather quickly following the onset of flow, with an approximate local steady-state being established by $t \approx 0.2$ (some smaller changes are observed to occur at later times, see below).

In contrast to the rapid density changes observed close to the wall, the migration of particles in the non-uniform Poiseuille flow occurs much more slowly. In

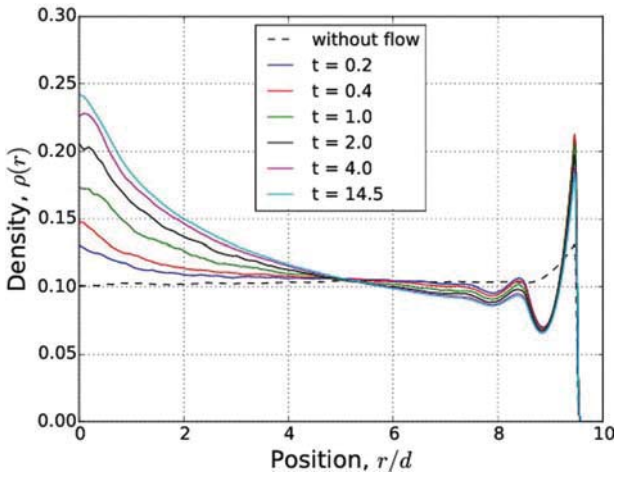

Figure 3. As in Figure 2, but focusing on the central peak region (around $r = 0$) and for later times following the onset of flow. For increasing time we see a monotonic increment of the central peak.

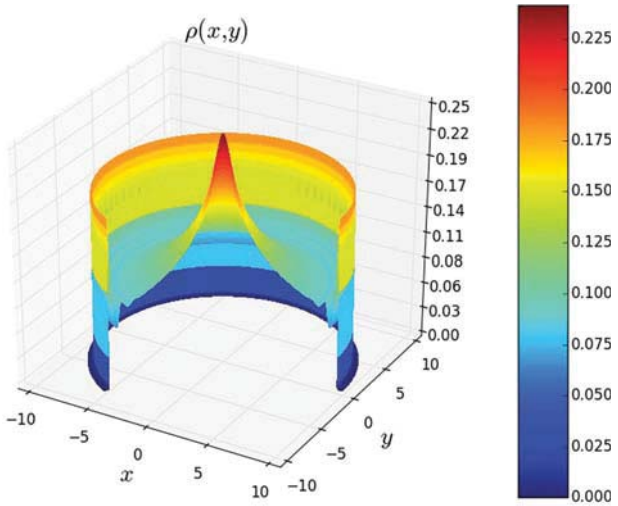

Figure 4. Three-dimensional visualisation of the steady-state data shown in Figure 3. Peclet number $Pe = 250$.

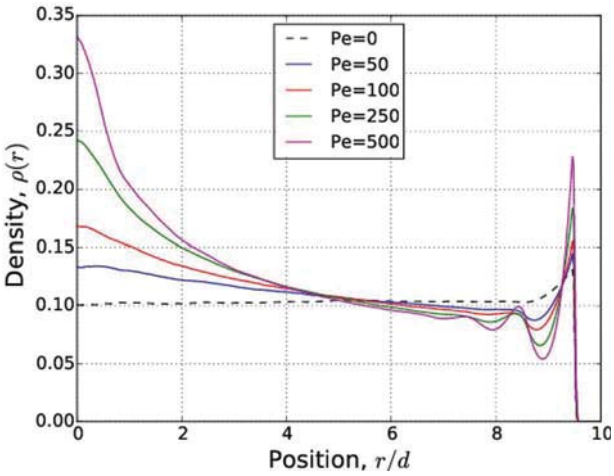

Figure 5. The Peclet number dependence of the steady-state density for monodisperse repulsive-spheres confined in a cylindrical geometry. We see a monotonic increment of the central peak.

Figure 3, we show the time-evolution of the full radial density profile. The earliest density profile shown in the figure is for $t = 0.2$, by which time the structure close to the wall is approximately in the steady-state. As time progresses further we observe a gradual drift of particles towards the centre of the pipe, driven by the migration mechanism described earlier. The migration peak at the centre of the density profile eventually saturates at around $t = 15$. The growth of this peak is a slow process, which requires material to be transported from the periphery of the pipe towards the centre. This transport depletes the density in the wall region and leads to slight modification of the oscillatory structure of the profile with increasing time. As the migration peak builds up, the emerging density gradient starts to counteract the migration force until a steady-state balance is eventually achieved. We find that the growth of the central peak as a function of time can be well approximated by an exponential.

In Figure 4, we show a three-dimensional representation of the steady-state profile (corresponding to the light-blue line in Figure 3). Due to the cylindrical symmetry of the problem this representation does not provide additional information. However, in our opinion, it does provide a stronger intuitive impression of how the particles are distributed within the pipe. An important conclusion to be drawn from these simulations is that establishing a steady-state migration peak requires approximately two orders of magnitude more time than the local rearrangements close to the wall. There is a clear separation of time-scales. Although we have only shown data for a single volume fraction, we have checked that the same conclusion can be drawn over a wide range of volume fractions and shear-rates.

We next consider the influence of the shear-rate on the steady-state density profiles. In Figure 5, we report the steady-state density profiles for Peclet numbers ranging from $Pe = 0$ to 500. As expected, both the layering at the wall and the migration effect are enhanced by increasing the Peclet number; however, we also observe that the functional form of the profile changes in character in going from low to high Pe. At low values of Pe the decrease in density from the pipe centre towards the wall is an approximately linear function of the radial position, whereas for values of Pe greater than around 200 a significant curvature develops. For the volume fraction under consideration, $\phi = 0.05$, we observe that the central peak height increases sublinearly as a function of Pe, eventually saturating at very high values of Pe (although

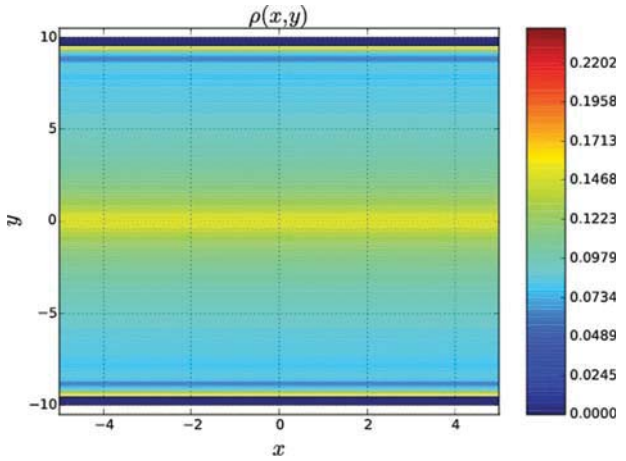

Figure 6. A two-dimensional representation (projection) of our three-dimensional data for the steady-state density profile in a channel geometry with flow in the *x*-direction and shear gradient in the *y*-direction. $Pe = 250$.

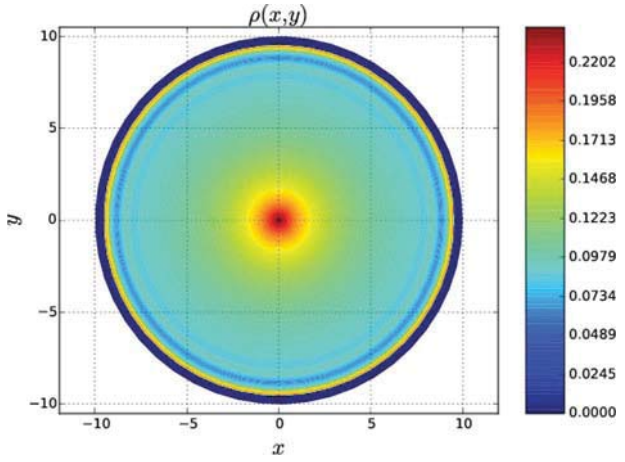

Figure 7. A two-dimensional representation (projection) of our three-dimensional data for the steady-state density profile in a cylindrical geometry. $Pe = 250$.

very large Peclet numbers were not systematically investigated). While these observations remain valid for low to intermediate volume fraction suspension, for dense liquid states ($\phi \geq 0.4$) the picture becomes different. For such dense systems the density around the pipe centre becomes much less sensitive to increasing *Pe*, as many-particle packing effects interfere with and disrupt the migration mechanism [20].

As the two most commonly studied, and physically relevant, geometries are cylindrical and planar (slit) confinement, it is of interest to compare the density profiles obtained in each case for equal values of the simulation parameters. In order to have a significant migration peak in steady-state, we will fix the Peclet number for this comparison to the value $Pe = 250$. The cylindrical system remains the same as that reported above. For the simulation of the planar system, we have used the following parameters: the number of particles $N = 250$, the box size $L_x = 10d$, $L_y = 20d$ and $L_z = 13.09d$ and again a Brownian time step $dt = 2 \times 10^{-5}$. The external flow acts in the z-direction with shear-gradient in the y-direction. In Figure 6, we show the projected steady-state profile in the velocity-gradient plane. As expected, in the planar geometry the colloids are driven towards the central ($y = 0$) line by the migration mechanism. As a phenomenological comparison, we report in Figure 7 the same situation for the system under cylindrical confinement. It is apparent from the colour bar that the migration is relatively stronger in the cylindrical geometry than it is in the channel geometry. This effect is due to the fact that the migrational drift of the particles is 'focused' on a central point (in our projected representation) instead of on a central line.

3.2. Bidisperse and polydisperse systems

We now consider the case of a bidisperse system of spheres, interacting via the same pair potential as used in the previous section, but now with two species of different diameter, d_1 and d_2. The simulation parameters used here are: the total number of particles $N = 400$, the Brownian time step $dt = 5 \times 10^{-6}$, the length of pipe $L = 13.125d$, the maximal fluid velocity $v_m = 2500$, number of particles of species 1 $N_1 = 200$ and the number of particle of species 2 $N_2 = 200$.

An interesting possibility which arises for this system is whether there exist conditions for which the migration effect can be reversed for one of the species, thus generating a steady-state with a density minimum at the centre of the pipe. This effect has been demonstrated experimentally by Aarts *et al.* [24] for a mixture of red blood cells and platelets. Given that the driving force underlying the migration of particles is provided by an asymmetric distribution of colloidal collisions on the surface of a given particle, it follows intuitively that one would expect the larger of the two species to experience a stronger migration force than the smaller, which are consequently depleted from the region at the pipe centre. These expectations are validated by the data shown in Figure 8, for which we have simulated a system with $d_1 = 0.25d$ and $d_2 = 1.25d$. The main figure shows both density profiles on the same scale, whereas the inset focuses only on the second (smaller) species. The depletion in density at the centre of the pipe is of the order of around 5% of the bulk density for the parameters employed (the effect can be further enhanced by increasing the flow rate). We have found that decreasing the size-ratio of small to large spheres from unity to a value of around 0.2

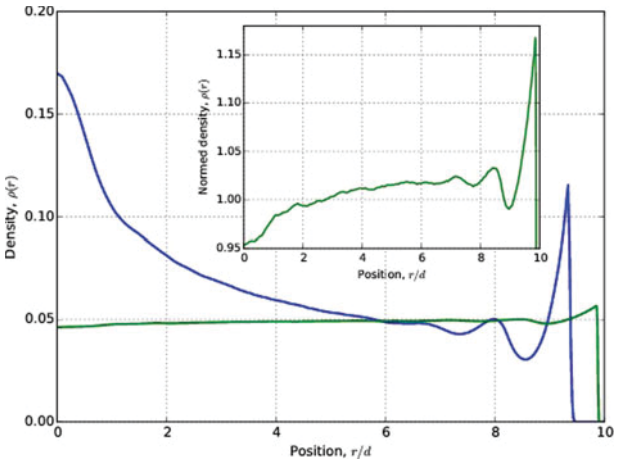

Figure 8. Reporting the higher peak, the size class $d_2 = 1.25d$ and relatively flat, the size class $d_1 = 0.25d$. In the inset, the density profile of the class d_1, renormalised by the bulk density.

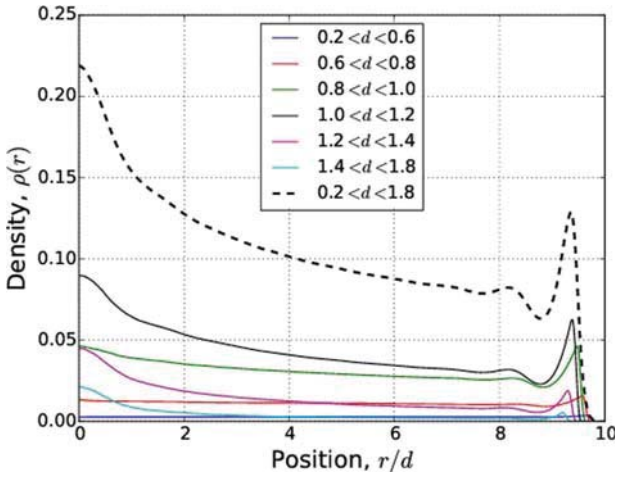

Figure 9. Steady-state density profiles for polydisperse repulsive-spheres with polydispersity $0.2d$ and average diameter equal to unity under Poiseuille flow with maximal velocity $v_m = 2500$.

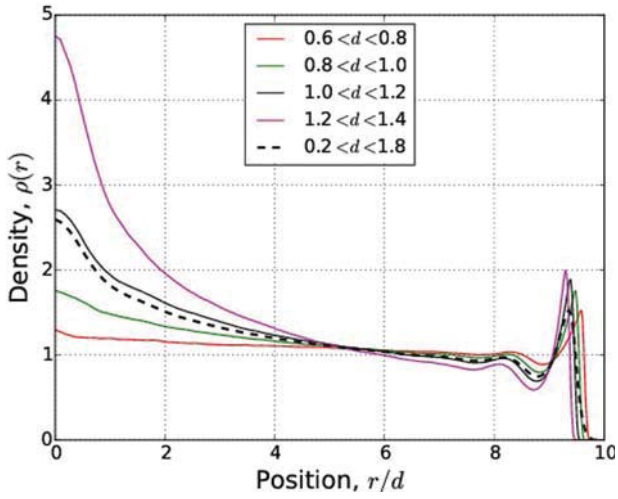

Figure 10. The same data as shown in Figure 9 normalised according to the bulk density of each size class. The central peak height decreases monotonically with decreasing particle size.

leads to an increase in the magnitude of the small particle depletion at the pipe centre. However, for smaller size ratios the large spheres are less efficient in excluding the smaller ones from the central region, as the latter can pass through the 'gaps' between larger spheres, and the depletion effect becomes less prominent.

From these results we can conclude that an anti-migration phenomenon can be obtained in bidisperse mixtures, provided that the size ratio, d_2/d_1, is not too small (smaller than around 0.2). This spatial separation of the two species could, for example, be exploited for the separation of biological fluids, where one could extract one species of particle at the boundary and the other from the centre of the pipe.

We next consider a polydisperse system with a continuous distribution of particle sizes. For convenience we select the particle diameters from a Gaussian distribution with standard deviation $0.2d$ and average equal to unity. Due to the difference in the particle sizes, one has to adapt the Brownian velocity accordingly. The standard deviation of the Brownian generator takes now the form $\hat{\sigma}_i = \sqrt{d_0 2T' dt/d_i}$, where d_0 is the reference diameter, here $d_0 = 1$, and d_i is the diameter of particle i. The simulation parameters to be used for our polydisperse simulations are: number of particles $N = 400$, length of the pipe $L = 15.07d$, Brownian time step $dt = 10^{-5}$ and the maximal velocity of the background fluid $v_m = 2500$.

As we are now dealing with a continuous size distribution it is useful to divide the particles into different size classes, e.g. those particles with diameter between $0.8d$ and d, in order to aid the graphical presentation of our numerical data. In Figure 9, we show the average density profiles for different size classes, together with the total density profile obtained by summing all of the individual classes. As expected, the total density displays a clear migration peak at the pipe centre, similar in form to the density of the monodisperse system at a comparable volume fraction. However, the oscillations close to the boundary are less pronounced than in the monodisperse case, because the polydispersity frustrates the particle packing.

The relative influence of migration on the different particle size classes is made more clear in Figure 10, where we show each of the profiles normalised by the appropriate bulk density. If we take the data for the total density (broken line in the figure) to represent the average migration profile of the particles, then it is clear that the classes containing the larger particles exhibit

a much stronger migration peak than those containing the smaller particles. This is consistent with our findings from the bidosperse system. If we recall the definition of the Peclet number, ($Pe = \frac{v_m d^2}{RD_0}$) we can rationalise these observations: the bigger particles experience a larger Peclet number than the smaller ones, and are thus driven more effectively to the centre of the pipe.

3.3. Mono-disperse Lennard-Jones spheres

The purely repulsive interactions so far considered can be realised using certain, specially prepared model systems (e.g. PMMA spheres). However, in general, colloids in suspension also exhibit an attractive component to their interaction potential. It is thus somewhat surprising that to date there have been no studies of the influence of interparticle attraction on the steady-state density profiles in Poiseuille flow. In equilibrium, attractive systems demonstrate phase separation into colloid-rich and colloid-poor phases. In the present nonequilibrium situation it is not clear how the cohesive tendency of the particles will interact with the migration mechanism. On one hand, the development of a migration peak might be expected to be favoured, as the formation of dense regions would lead to a lowering of the systems potential energy. On the other hand, it is not clear how the migration mechanism itself (which generates the density peak) is altered when the particles prefer to stick together: an excess of collisions on one side of a particle surface could give rise to a 'pull' towards the walls, rather than an inwards 'push', as is the case for purely repulsive interactions.

The simulations have been performed using the following parameters: the number of particles $N = 400$, the length of the pipe $L = 13.33d$ and the Brownian time step $dt = 2 \times 10^{-5}$. The interparticle interaction potential takes the well-known form

$$U_{\mathrm{LJ}} = 4\epsilon \left[\left(\frac{d}{r}\right)^{12} - \left(\frac{d}{r}\right)^{6} \right]. \qquad (3)$$

For the wall-particle interaction we retain the same repulsive potential used previously. In Figure 11, we show the steady-state density profile of a system formed by pseudo-hard spheres and LJ spheres. The main observation to be made here is that the central migration peak is higher for attractive particles than for repulsive particles. This enhancement can be made larger by increasing ε (the attraction strength) beyond the value $\varepsilon = 0.5$ considered in Figure 11. However, one should be careful to remain at ε values away from the two-phase region of the LJ phase diagram. Increasing the value beyond $\epsilon \approx 1$ complicates the situation by incorporating the physics of

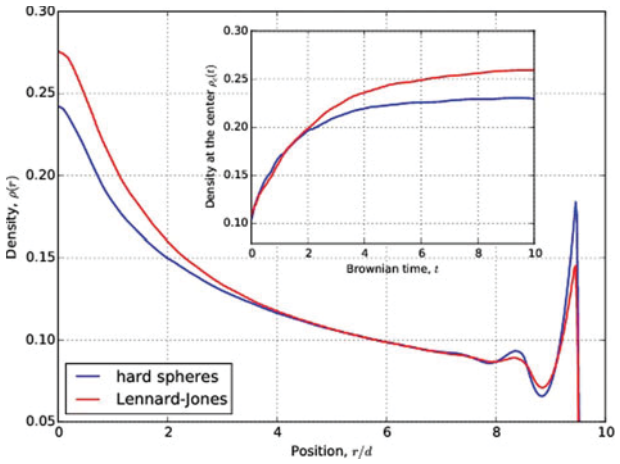

Figure 11. Comparison of the steady-state density profile of repulsive particles with that of attractive Lennard-Jones particles. The attraction parameter $\epsilon = 0.5$ and the Poiseuille flow are the same as that considered in the previous figures. In the inset we show the height of the central peak as a function of the time since the onset of flow.

phase separation dynamics. Although we have not studied these effects in detail we do find significant sensitivity of the steady-state profiles to ϵ in the vicinity of the binodal.

In the inset of Figure 11, we show the value of the central density peak as a function of the time since the onset of flow. The steady-state is achieved slightly faster for the repulsive system than for the attractive system. We note that the initial growth of the peak height is virtually identical for the first two Brownian time units. Recalling that we are working at rather low-volume fractions, this suggests that the mechanism of migration, on the level of binary collisions, is not significantly different in the two systems. However, for later times the density in the central region becomes sufficiently large that the interparticle attraction causes the particles to pull together, enhancing the height of the peak.

3.4. Polydisperse Lennard-Jones spheres

In order to bring our investigations somewhat closer to experimental reality, we now consider the steady-state profiles of polydisperse LJ particles. As previously, we will employ a Gaussian distribution of particle sizes and compare our results for the attractive system with those previously obtained for the purely repulsive system. The results are represented in Figure 12 for a maximal velocity of $v_m = 2500$.

For each size class the migration peak is enhanced by turning on the attraction, but this enhancement is most pronounced for the larger particles. This suggests that interparticle attraction could be used to increase

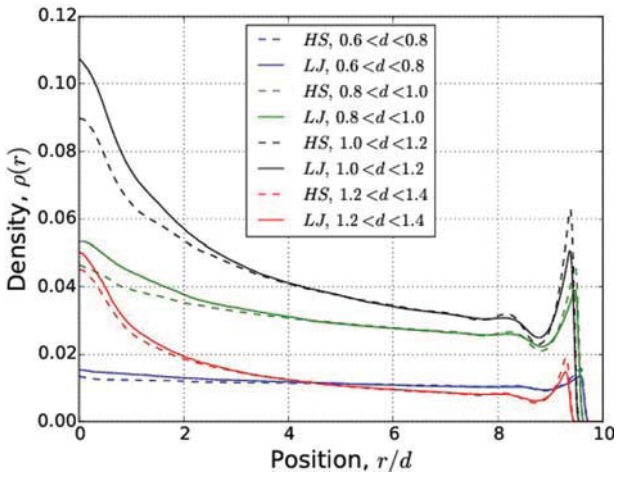

Figure 12. Comparison of the steady-state density distribution of a system of polydisperse, attractive (Lennard-Jones) particles with that of a system of polydisperse, repulsive particles. Both systems are characterised by a polydispersity 0.2*d* and average of *d*. The Lennard-Jones attraction parameter is set to $\epsilon = 0.5$.

yield efficiency of devices which segregate the particles according to their size. The first packing peak at the wall decreases with increasing attraction, because our choice of repulsive substrate tends towards drying, rather than wetting, as the attraction is increased.

4. Conclusions

In this paper, we have presented a simulation study of shear-induced migration in monodisperse, bidisperse and polydisperse systems subject to Poiseuille flow. For repulsive interparticle interactions, we find that the migration- induced density peak at the centre of the channel develops much more slowly (around two orders of magnitude, for the parameters considered) than local structural changes close to the channel boundaries. For monodisperse systems, we have shown that the steady-state accumulation of particles at the centre of the channel is more pronounced in cylindrical geometry than in planar geometry. For systems of polydisperse repulsive particles we find that the migration effect is strongest for the larger particles, suggesting that migration could possibly be exploited as a mechanism for sorting or separating particles according to their size. In the special case of a bidisperse system we find that it is possible to induce an 'anti-migration' effect in the smaller size particles, whereby their density is depleted, rather than enhanced, in the central region of the channel.

By considering systems of LJ particles, we have addressed the influence of interparticle attractions on the steady-state density profiles. We note that care was taken to consider only parameters for which bulk phase separation does not occur. We find that adding an interparticle attraction enhances the height of the central density peak in steady-state, both for monodisperse and polydisperse systems, and could then be used as a means to optimise particle segregation effects in potential applications. However, the transient dynamics in going from equilibrium to steady-state are not strongly influenced by the presence or absence of attraction.

There are several possibilities to extend the findings of the present work. In Refs. [6,15], a dynamical density functional theory was developed, which incorporates the physics of shear-induced migration in a mean-field fashion. It would be interesting to exploit the numerical data presented in this work to optimise the approximations employed in the theory – particularly for the case of attractive interparticle interactions. In this work, we have focused exclusively on systems with a strongly repulsive core. However, there is also much interest in model systems for which the particles interact via soft, penetrable interactions (modelling, e.g. polymer coils). Whether the picture of migration presented here holds also for these systems remains an open question. Finally, it seems to us possible that, should the migration lead to a sufficiently enhanced density at the channel centre, then crystallisation effects could start to play a role: can a steady-state crystal structure be induced by non-uniform flow? We will continue to investigate these and related phenomena.

Disclosure statement

No potential conflict of interest was reported by the authors.

Funding

We thank the Swiss National Science Foundation for financial support [grant number 200021_153657/2].

References

[1] J.M. Brader, J. Phys. : Condens. Matter. **22**, 363101 (2010).
[2] J.K.G. Dhont, M.P. Lettinga, Z. Dogic, T.A.J. Lenstra, H. Wang, S. Rathgeber, P. Carletto, L. Willner, H. Frielinghaus and P. Lindner, Faraday Discuss. **123**, 157 (2003).
[3] R. Besseling, L. Isa, P. Ballesta, and W. Poon, Phys. Rev. Lett. **105**, 268301 (2010).
[4] H. Jin, K. Kang, K.H. Ahn and J.K.G. Dhont, Soft. Matter. **10**, 9470 (2014).
[5] F. Varnik, L. Bocquet, J.-L. Barrat and L. Berthier, Phys. Rev. Lett. **90**, 095702 (2003).
[6] J.M. Brader and M. Krüger, Mol. Phys. **109**, 1029 (2011).
[7] D.R. Foss and J.R. Brady, J. Rheol. **44**, 629 (2000).
[8] D. Semwogerere and E.R. Weeks, Phys. Fluids **20**, 043306 (2008).

[9] A. Kumar and M.D. Graham, Soft. Matter. **8**, 10536 (2012).
[10] K.L. McCarthy and W.L. Kerr, J. Food Eng. **37**, 11 (1998).
[11] F. Gadala-Maria and A. Acrivos, J. Rheol. **24**, 799 (1980).
[12] D. Leighton and A. Acrivos, J. Fluid. Mech. **181**, 415 (1987).
[13] P. Nozieres and D. Quemada, Europhys. Lett. **2**, 129 (1986).
[14] R.J. Phillips, R.C. Armstrong, R.A. Brown, A.L. Graham and J.R. Abbott, Phys. Fluids A. **4**, 30 (1992).
[15] A. Scacchi, M. Krüger and J.M. Brader, J. Phys.: Condens. Matter. **28**, 244023 (2016).
[16] P.R. Nott and J.F. Brady, J. Fluid Mech. **275**, 157 (1994).
[17] J.F. Morris and J.F. Brady, Int. J. Multiphase Flow **24**, 105 (1998).
[18] A. Acrivos, R. Mauro, and X. Fan, Int. J. Multiphase Flow **19**, 797 (1993).
[19] M. Frank, D. Anderson, E.R. Weeks, and J.F. Morris, J. Fluid. Mech. **493**, 363 (2003).
[20] M.K. Lyon and L.G. Leal, J. Fluid. Mech. **363**, 25 (1998).
[21] M.K. Lyon and L.G. Leal, J. Fluid. Mech. **363**, 57 (1998).
[22] D. Katanov, G. Gompper, and d.A. Fedosov, Microvasc. Res. **99**, 57 (2015).
[23] M.P. Allen and D.J. Tildesley, *Computer Simulation of Liquids* (Clarenden Press, Oxford, 1989).
[24] P.A.M.M. Aart, S.A.T. van den Broek, G.W. Prins, G.D.C. Kuiken, J.J. Sixma, and R.M. Heethaar, Arterioscler. Thromb. Vasc. Biol. **8**, 819 (1988).